tvst

Glaucoma

Relationship Between Deep Retinal Macular Vessel Density and Bipolar Cell Function in Glaucomatous Eyes

Yuji Yoshikawa[1], Takuhei Shoji[1], Junji Kanno[1], Hirokazu Ishii[1], Minami Chino[1], Yuro Igawa[1], Kei Shinoda[1], and Yozo Miyake[2]

[1] Department of Ophthalmology, Saitama Medical University, Saitama, Japan
[2] Kobe City Eye Hospital, Hyogo, Japan

Correspondence: Kei Shinoda, Department of Ophthalmology, Saitama Medical University, 38 Moro-Hongo Moroyama-machi, Iruma-gun, Saitama 350-0495, Japan. e-mail: shinodak@med.teikyo-u.ac.jp

Received: February 11, 2022
Accepted: September 6, 2022
Published: October 3, 2022

Keywords: glaucoma; vessel density; multifocal electroretinogram; optical coherence tomography angiography; bipolar cells

Citation: Yoshikawa Y, Shoji T, Kanno J, Ishii H, Chino M, Igawa Y, Shinoda K, Miyake Y. Relationship between deep retinal macular vessel density and bipolar cell function in glaucomatous eyes. Transl Vis Sci Technol. 2022;11(10):4, https://doi.org/10.1167/tvst.11.10.4

Purpose: To evaluate the correlation between macular retinal function and the changes in the macular retinal vascular structure in glaucomatous eyes.

Methods: The study included patients with glaucoma who visited Saitama Medical University and underwent optical coherence tomography angiography, and multifocal electroretinographic examinations at the same time between February 2020 and April 2021. Correlations among the ocular parameters, macular vessel density, and multifocal electroretinographic parameters were evaluated using a mixed model.

Results: Forty-one eyes (mean deviation, -12.4 ± 7.8 dB) of 24 subjects (mean age, 75.2 ± 8.3 years) were included in the analysis. There were no significant correlations for macular vessel density in the superficial retinal layer. However, macular vessel density in the deep retinal layer showed a significant positive correlation with P1–N1 amplitude (coefficient $= 0.724$; $P = 0.001$). There were no significant correlations between the optical coherence tomography parameters and any of the multifocal electroretinographic parameters.

Conclusions: A decrease in N1–P1 amplitude was observed in glaucomatous eyes in relation to a reduction in macular vessel density in the deep retinal layer, which suggests that ischemia-induced bipolar cell dysfunction may be involved in the intermediate retinal dysfunction associated with glaucoma.

Translational Relevance: Intermediate retinal dysfunction in glaucoma is related to the changes in deep retinal microvasculature.

Introduction

Glaucoma is a chronic progressive disease and one of the leading causes of blindness worldwide.[1–3] Early diagnosis, control of intraocular pressure, and monitoring the progress to determine whether additional topical medications or surgery are indicated play a crucial role in the successful management of glaucoma. Two theories have been proposed for the development of glaucoma. The first theory suggests that high intraocular pressure causes mechanical damage to the retinal nerve fiber layer at the level of the lamina cribrosa, leading to the development of glaucoma (mechanical theory). The second theory suggests that insufficient ocular blood supply, including retinal and choroidal circulation, leads to the development of glaucoma (vascular theory).[4–6]

Studies on glaucoma using optical coherence tomography angiography (OCTA) have shown changes in the vascular structure of the optic nerve head, including optic disc vessel density (VD),[7,8] superficial peripapillary VD,[9,10] and peripapillary deep choroidal VD.[11] Moreover, other OCTA studies have shown changes in the superficial retinal VD in the macular area, where retinal ganglion cells are distributed.[12,13]

However, our recent studies have shown that glaucomatous eyes with central visual field (VF) defects show changes in the deep macular microvasculature.[14] Another study showed that macular VD in the

deep capillary plexuses decreased significantly more rapidly in eyes with primary open-angle glaucoma and high myopia than in those without high myopia.[15] However, the causal relationship between the deep retinal vascular structure, which is distributed in the inner nuclear layer (INL) and the outer plexiform layer, and glaucoma, a disorder of the inner retinal layer represented by retinal ganglion cells, remains unclear.

Previous studies using optical coherence tomography (OCT) have reported that glaucomatous eyes may also show alterations in the outer retinal layer.[16–19] Further studies using full-field electroretinography and multifocal electroretinography (mfERG) have shown that glaucomatous eyes exhibit a-wave, b-wave, and P1 attenuation.[20–23] There is no clear consensus regarding the reasons for these findings. In this study, we evaluated macular retinal function using mfERG and tested for its correlation with the corresponding changes in the macular retinal vascular structure in glaucomatous eyes.

Methods

Study Design

This retrospective cross-sectional study was approved by the ethics committee of Saitama Medical University, Iruma, Japan (approval number 2021-56) and adhered to the tenets of the Declaration of Helsinki. Written informed consent was obtained from all study participants after they were provided with an explanation of the nature and possible consequences of the study.

Study Subjects and Examinations

Patients with glaucoma who visited Saitama Medical University and underwent OCTA and mfERG examinations on the same day between February 1, 2020, and April 22, 2021, were included in the study. Glaucoma was diagnosed using the established criteria,[14] which require the presence of at least one of the following: glaucomatous optic neuropathy, repeatable abnormal standard automated perimetry results, abnormal glaucoma hemifield test results, or pattern standard deviation values outside the normal limits. Patients and eyes were excluded if any of the following were present: a history of intraocular surgery (except for cataract or glaucoma surgery), non-glaucomatous optic neuropathy, vascular or nonvascular retinopathy, or another ocular or systemic disease known to impair VF. All participants underwent comprehensive ophthalmic examinations, including assessment of best-corrected visual acuity (Landolt chart), slit-lamp biomicroscopy, measurement of intraocular pressure (Goldmann applanation tonometry), fundus photography (CX-1; Canon, Inc., Tokyo, Japan), measurement of axial length and central corneal thickness (Optical Biometer OA-2000; Tomey Corp., Nagoya, Japan), and standard automated perimetry (Humphrey 24-2 Swedish Interactive Thresholding Algorithm; Carl Zeiss Meditec, Jena, Germany). In addition, all subjects underwent swept-source OCTA (SS-OCTA; PLEX Elite 9000, version 1.6.0.21130; Carl Zeiss Meditec) and spectral-domain OCT (SPECTRALIS HRA 2, Heidelberg Engineering, Heidelberg, Germany) to examine the thicknesses of the macular ganglion cell complex (mGCC) and the macular inner nuclear layer-outer plexiform layer (mINOPL). Self-reported medical histories were extracted from the medical records, including the presence or absence of hypertension, diabetes, and hyperlipidemia.

OCTA Examination of mVD

All SS-OCTA examinations were performed within a 6 × 6-mm (300 × 300 pixels) volume scan centered on the fovea. The SS-OCTA system had a central wavelength of 1060 nm, an A-scan rate of 100,000 scans/s, and axial and transverse tissue resolution of 6.0 and 20.0 µm, respectively. The angiographic images were processed using both phase/Doppler shift and amplitude variation (optical micro-angiography).[24] All SS-OCTA en face images of the superficial retinal layer (SRL), which is between the inner surface of the internal limiting membrane layer and the outer surface of the inner plexiform layer, and the deep retinal layer (DRL), which is between the inner surface of the inner plexiform layer and the outer surface of the outer plexiform layer, were automatically obtained and analyzed using built-in segmentation software. The DRL OCTA images were also analyzed using built-in projection artifact-removal software. Images with segmentation failure, artifacts, or off-centered positioning were excluded from the analyses.

Macular vessel density (mVD) was measured within a circle with an outer diameter of 6 mm and was calculated for SRL and DRL. Angiography signals were subjected to Otsu analysis[25] for OCTA image binarization using ImageJ (National Institutes of Health, Bethesda, MD) to obtain microvascular signals. VD was then calculated as the percent area occupied by the vessels (i.e., the angiography signal area relative to the concentric circle area), which has shown excellent reproducibility (Fig. 1).[26]

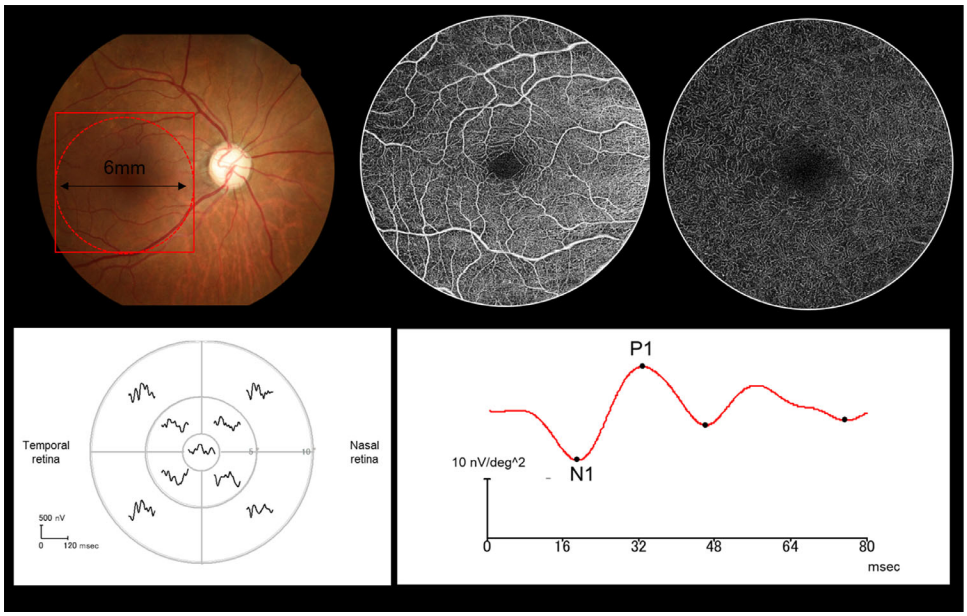

Figure 1. OCTA and mfEGR analyses were performed for a circle of 6 mm in diameter centered on the fovea. OCTA images measuring 6 mm × 6 mm were obtained to calculate the vessel density inside the circle measuring 6 mm in diamete for both the superficial and deep retinal layers. For mfERG, nine elements within a 20° diameter were stimulated, and the amplitude and latency of P1 and N1 were measured from the additive waveforms inside the concentric circles.

Multifocal Electroretinogram Examination

The mfERG test was performed using an LE-4100 system (Mayo Corporation, Inazawa, Japan) under ordinary room illumination with a natural pupil. The stimuli were displayed with a digital light processing projector and consisted of nine elements arranged in a dart pattern with an overall diameter of 3.37°, 10.1°, or 20.2°.[27] They were designed to record a focal response from the retina corresponding to the OCTA examination (i.e., the Early Treatment of Diabetic Retinopathy Study chart areas) (Figs. 1, 2) and to illustrate the stimulus on the monitor. Figure 1 shows the focal ERGs and the area stimulated. An m-sequence was delivered at a rate of 75 frames/s and a cycle of 2^{13} – 1 steps, and stimulus intensity was 20 cd.s/m^2 (1500 cd/m^2 for white, 28 cd/m^2 for black).

A red fixation cross was positioned across the entire stimulus screen, and the subjects were instructed to fixate on the crosspoint or the center of the screen and resist blinking. The best refractive correction was used for each subject, and all recordings were monocular. The signals were detected by a silver plate electrode placed on the lower eyelid as an active electrode, amplified (×248), bandpass filtered (10–60 Hz at half-amplitude), and digitalized at a 1200-Hz sampling frequency. The recording time was 1 minute, 49 seconds. The reference electrode was placed on the lower eyelid of the opposite eye, and the ground electrode was placed on the earlobe. The amplitude and latency of the N1 wave and the N1–P1 amplitude and latency of the P1 wave were measured in a circle at 20° in the central fovea (Figs. 1, 2).

Data Analysis

We assessed the distribution of numerical variables by inspecting histograms and using the Shapiro–Wilk W test of normality. Normally distributed variables are reported as the mean ± standard deviation (SD). Non-normally distributed variables are reported as the median (quartiles). The correlations among the ocular parameters, mVD, and mfERG parameters were evaluated using a mixed model. All statistical analyses were performed using JMP 10.1 (SAS Institute, Cary, NC) and STATA 16 (Stata Corp., College Station, TX). $P < 0.05$ was considered statistically significant.

Results

Twenty-six patients with mono- or binocular glaucoma were initially enrolled in the study. After excluding seven eyes with epiretinal membrane, two eyes with retinal vein occlusion, and two eyes without glaucoma, 41 glaucomatous eyes of 23 patients were eligible for the analysis. The patients had a mean age

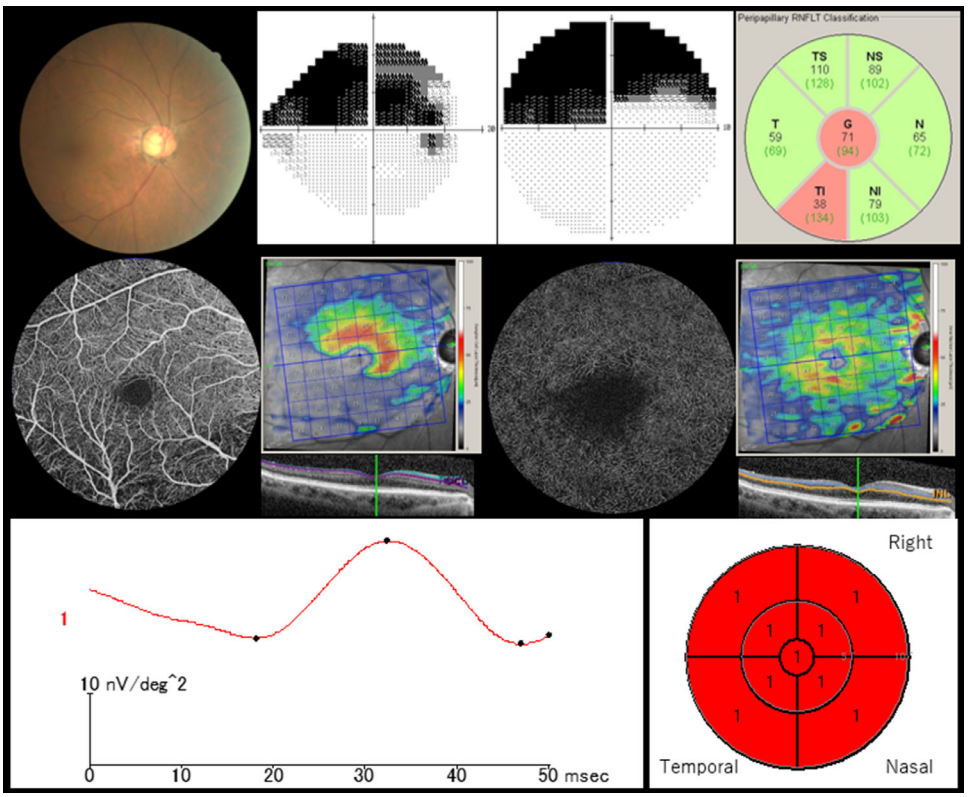

Figure 2. Representative cases. There is inferior thinning of the retinal nerve fiber layer and ganglion cell layer with corresponding superior visual field loss. OCTA images show loss of superficial vascular signals corresponding to the de-thinned area of the ganglion cell layer. The OCTA image of the deep retinal layer showed attenuation and dropout of vascular signals in proximity to the lower foveal avascular zone. The multifocal electroretinogram waveform was analyzed inside a concentric circle with a 6-mm diameter, corresponding to the OCTA analysis area.

of 75.2 ± 8.3 years, and the mean deviation (MD) was −12.4 ± 7.8 dB. Table 1 presents the OCT and OCTA parameters: mGCC thickness, 74.0 ± 13.0 µm; mINOPL thickness, 58.8 µm (quartiles, 56.1–60.1); SRL-mVD, 38.2% (quartiles, 35.5–40.5); and DRL-mVD, 53.3% (quartiles , 42.7–56.7). The N1 amplitude was −5.50 ± 2.19 nV/deg^2, the N1–P1 amplitude was 11.4 ± 4.9 nV/deg^2, the N1 latency was 17.6 ± 2.8 ms, and the P1 latency was 33.1 ± 2.2 ms (Table 1).

The scatterplots (Supplementary Figs. S1–S5) showed a significant positive correlation between SRL-VD and mGCC thickness (R^2 = 0.157, P = 0.010), a significant positive correlation between DRL-VD and N1-P1 amplitude (R^2 = 0.444, P < 0.001), and a significant negative correlation between DRL-VD and N1 amplitude (R^2 = 0.146, P = 0.014). Furthermore, N1–P1 amplitude and INOPL thickness showed a significant positive correlation (R^2 = 0.184, P = 0.005).

In univariate analysis (mixed model), SRL-mVD was significantly correlated with age (coefficient = −0.229, P = 0.007), best-corrected visual acuity (logMAR; coefficient = −22.3, P < 0.001), MD (coefficient = 0.120, P = 0.006), and mGCC thickness

Table 1. Eye Parameters (N = 41)

Parameter	
Ocular parameters	
Age (y), mean ± SD	75.2 ± 8.3
Sex (female/male), *n*	23/18
IOP (mmHg), mean (range)	13.7 (10.2 to 17.2)
BCVA (logMAR), mean (range)	−0.08 (−0.08 to 0.10)
Axial length (mm), mean (range)	23.7 (22.7 to 25.3)
SE (D), mean ± SD	−1.3 ± 2.6
MD value (dB), mean ± SD	−12.4 ± 7.8
Self-reported history of systemic disease, %	
Hypertension	34.1
Diabetes	9.8
Hyperlipidemia	19.5
OCT parameters	
mGCC thickness (µm), mean ± SD	74.0 ± 13.0
mINOPL thickness (µm), mean (range)	58.8 (56.1 to 60.1)
OCTA parameters	
SRL-mVD (%), mean (range)	38.2 (35.5 to 40.5)
DRL-mVD (%), mean (range)	53.3 (42.7 to 56.7)
mfERG parameters, mean ± SD	
N1 latency (m/s)	17.6 ± 2.8
N1 amplitude (nV/deg^2)	−5.50 ± 2.19
P1 latency (m/s)	33.1 ± 2.2
N1–P1 amplitude (nV/deg^2)	11.4 ± 4.9

IOP, intra ocular pressure; BCVA, best-corrected visual acuity; SE, spherical equivalent.

Table 2. Correlation Coefficients for SRL–mVD (Mixed Model)

	Univariate Analysis		Multivariate Analysis	
	Correlation Coefficient (95% CI)	*P*	Correlation Coefficient (95% CI)	*P*
Ocular and systemic parameters				
Age (y)	−0.229 (−0.394 to −0.063)	0.007	−0.021 (−0.177 to 0.135)	0.792
Sex (ref. male)	1.118 (−2.062 to 4.264)	0.486	—	—
SE (D)	0.091 (−0.503 to 0.686)	0.764	—	—
BCVA	−22.32 (−29.63 to −15.00)	<0.001	−10.37 (−21.16 to 0.411)	0.059
Axial length (mm)	0.275 (−0.907 to 1.458)	0.648	—	—
IOP (mmHg)	0.158 (−0.029 to 0.346)	0.099	—	—
MD value (dB)	0.120 (0.059 to 0.341)	0.006	0.085 (−0.100 to 0.272)	0.366
Self-reported history of hypertension	2.680 (−0.462 to 5.822)	0.095	—	—
Self-reported history of diabetes	−2.874 (−8.174 to 2.427)	0.288	—	—
Self-reported history of hyperlipidemia	0.940 (−2.984 to 4.865)	0.639	—	—
OCT parameters				
mGCC thickness	0.132 (0.032 to 0.231)	0.009	0.023 (−0.079 to 0.126)	0.654
mINOPL thickness	−0.126 (−0.362 to 0.0108)	0.292	—	—
mfERG parameters				
N1 latency (ms)	0.296 (−0.181 to 0.773)	0.224	—	—
N1 amplitude (nV/deg^2)	−0.103 (−0.742 to 0.534)	0.751	—	—
P1 latency (ms)	−0.501 (−1.009 to 0.086)	0.094	—	—
N1–P1 amplitude (nV/deg^2)	0.012 (−0.289 to 0.312)	0.939	—	—

Table 3. Correlation Coefficients for DRL–mVD (Mixed Model)

	Univariate Analysis	
	Correlation Coefficient (95% CI)	*P*
Ocular and systemic parameters		
Age (y)	−0.097 (−0.461 to 0.267)	0.601
Sex (ref. male)	−2.785 (−9.055 to 3.484)	0.484
SE (D)	−0.043 (−0.903 to 0.823)	0.922
BCVA	−5.306 (−15.22 to 4.613)	0.294
Axial length (mm)	−0.074 (−2.274 to 2.124)	0.947
IOP (mmHg)	−0.076 (−0.266 to 0.114)	0.435
MD value (dB)	0.036 (−0.150 to 0.222)	0.705
Self-reported history of hypertension	0.265 (−6.457 to 6.988)	0.938
Self-reported history of diabetes	−2.163 (−13.53 to 9.201)	0.709
Self-reported history of hyperlipidemia	−0.080 (−7.904 to 7.744)	0.984
OCT parameters		
mGCC thickness	0.017 (−0.068 to 0.101)	0.697
mINOPL thickness	−0.085 (−0.282 to 0.115)	0.410
mfERG parameters		
N1 latency (m/s)	−0.059 (−0.533 to 0.414)	0.805
N1 amplitude (nV/deg^2)	−0.593 (−1.217 to 0.310)	0.063
P1 latency (m/s)	−0.179 (−0.694 to 0.338)	0.497
N1–P1 amplitude (nV/deg^2)	0.724 (0.304 to 1.144)	0.001

(coefficient = 0.132, $P = 0.009$). However, multivariate analysis (mixed model) did not reveal any significant correlations (Table 2). DRL-mVD showed a significant positive correlation with the P1–N1 amplitude (coefficient = 0.724, $P = 0.001$); however, there was no significant correlation with mINOPL thickness (coefficient = −0.085, $P = 0.410$) (Table 3). There was a significant correlation between mGCC thickness and the MD values (coefficient = −1.011, $P < 0.001$) (Table 4). However, there was no significant correlation

Table 4. Correlation Coefficients for mGCC Thickness (Mixed Model)

	Univariate Analysis		Multivariate Analysis	
	Correlation Coefficient (95% CI)	*P*	Correlation Coefficient (95% CI)	*P*
Ocular and systemic parameters				
Age (y)	−0.391 (−0.855 to 0.072)	0.098	—	—
Sex (ref. male)	2.382 (−5.475 to 10.23)	0.552	—	—
SE (D)	0.439 (−1.070 to 1.949)	0.569	—	—
BCVA	−33.76 (−58.93 to −8.588)	0.009	1.115 (−31.32 to 33.55)	0.946
Axial length (mm)	0.153 (−2.828 to 3.134)	0.92	—	—
IOP (mmHg)	0.191 (−0.333 to 0.716)	0.475	—	—
MD value (dB)	1.001 (0.576 to 1.427)	<0.001	1.011 (0.507 to 1.515)	<0.001
Self-reported history of hypertension	7.248 (−0.707 to 15.20)	0.074	—	—
Self-reported history of diabetes	−2.607 (−15.78 to 10.57)	0.698	—	—
Self-reported history of hyperlipidemia	−4.057 (−13.86 to 5.757)	0.417	—	—
mfERG parameters				
N1 latency (m/s)	0.127 (−1.221 to 1.470)	0.856	—	—
N1 amplitude (nV/deg^2)	0.153 (−1.783 to 2.089)	0.877	—	—
P1 latency (m/s)	−1.022 (−2.792 to 0.747)	0.257	—	—
N1–P1 amplitude (nV/deg^2)	0.010 (−0.787 to 0.807)	0.980	—	—

Table 5. Correlation Coefficients for mINOPL Thickness (Mixed Model)

	Univariate Analysis	
	Correlation Coefficient (95% CI)	*P*
Ocular and systemic parameters		
Age (y)	−0.022 (−0.253 to 0.209)	0.853
Sex (ref. male)	−0.657 (−4.499 to 3.185)	0.737
SE (D)	−0.279 (−1.002 to 0.445)	0.450
BCVA	−33.76 (−58.93 to −8.588)	0.269
Axial length (mm)	0.031 (−1.411 to 1.473)	0.967
IOP (mmHg)	−0.020 (−0.266 - 0.226)	0.873
MD value (dB)	0.065 (−0.193 to 0.323)	0.620
Self-reported history of hypertension	0.336 (−3.699 - 4.372)	0.870
Self-reported history of diabetes	3.674 (−2.666 to 10.01)	0.256
Self-reported history of hyperlipidemia	−3.015 (−7.647 to 1.616)	0.202
mfERG parameters		
N1 latency (m/s)	0.010 (−0.613 to 0.632)	0.976
N1 amplitude (nV/deg^2)	−0.095 (−0.993 to 0.809)	0.837
P1 latency (m/s)	−0.114 (−0.936 to 0.708)	0.785
N1–P1 amplitude (nV/deg^2)	0.193 (−0.186 to 0.572)	0.319

between the OCT parameters and mfERG parameters (Tables 4, 5).

Discussion

In the present study, DRL-mVD showed a significant positive correlation with N1–P1 amplitude within 20° of the macula. It has been reported that N1 originates from the cone cells, hyperpolarizing bipolar cells, and Müller cells, whereas P1 originates from the depolarizing bipolar cells, hyperpolarizing bipolar cells, and Müller cells,[28,29] suggesting that ischemia of the deep retinal layer in glaucomatous eyes may cause cellular damage to the bipolar cells distributed in the INL.

Most ERG studies on glaucomatous eyes have focused on the photopic negative response, which

is the negative wave that follows the photopic b-wave response.[30,31] The photopic negative response reflects the function of the retinal ganglion cells and is known to decrease in amplitude with an increase in the stage of glaucoma.[31,32] Because the superficial capillary plexus is located in the retinal ganglion cell layer,[33] it is relatively easy to understand the thinning of the ganglion cell-inner plexiform layer (GCIPL),[34] the decrease in superficial parafoveal VD,[12] and attenuation of the photopic negative response[31,32] in glaucoma. However, the changes in the outer retinal layer structure on OCT[19] and reduction in the deep retinal VD[14] are difficult to explain on the basis of damage to the inner retinal layer. mfERG, using skin electrodes, can evaluate macular function easily and noninvasively; therefore, it is possible to evaluate glaucoma and functional changes in the middle and outer retinal layers of the local retinal area.[35]

In this study, we investigated the relationship between the changes in the macular microvasculature and retinal function by measuring the response density in the central 20° circle of the mfERG and mVD in the 6-mm concentric circles of the macula corresponding to the central 20° circle area. Because the deep capillary plexus is distributed from the INL to the OPL,[33] it is possible that bipolar cell damage is caused by a decrease in blood supply due to a reduction in deep retinal VD.

Kim et al.[36] reported that INL thickness is negatively correlated with the severity of glaucoma. Although the scatterplots showed a significant correlation between N1–P1 amplitude and mINOPL thickness (Supplementary Fig. S5), the mixed models showed no significant correlation between mINOPL and DRL-mVD or N1–P1 amplitude. Hasegawa et al.[37] observed microcystic lesions in the INL in some glaucomatous eyes and reported that the INL in areas where microcystic lesions were present was thicker than that in areas where they were absent. We were unable to perform multiple OCT scans of the macula in all cases; however, none had microcystic lesions on the cross OCT scan of the macula. Furthermore, previous reports have shown that the thickness of the INL does not differ according to the stage of glaucoma.[36] Although the scatterplots showed significant correlation between mINOPL and N1-P1 amplitude, we could not detect it in the mixed model. This is possibly because we did not include cases with a thickened INL and included only glaucomatous eyes that were a homogeneous population in terms of INL thickness. Therefore, future studies should be performed to include normal eyes in order to clarify the relationships among mINOPL thickness, N1–P1 amplitude, and DRL-mVD.

Although the presence of ischemia in INL and OPL may impair bipolar cell function, resulting in decreased N1–P1 amplitude, it is unclear whether the INL impairment is the result of the decreased deep retinal VD, or the decreased deep retinal VD is secondary to the INL impairment.

This study has several limitations. First, this was a cross-sectional study with a small number of cases. Second, no data were collected for normal eyes because of the retrospective nature of the study. The study was retrospective and did not compare patients to normals; thus, no observations were possible to see if similar findings might be seen in normal subjects. Future prospective study including normal controls is necessary to further reduce any bias. The third limitation is that the macular function was assessed using mfERG, not focal macular ERG. The mfERG is shaped largely by bipolar cell activity with smaller contributions from the photoreceptor, amacrine, and ganglion cells.[28,38,39] The function of the amacrine and ganglion cells may have been underestimated in the current study; thus, precise layer-by-layer analysis using focal macular ERG and their correlation with microvasculature using OCTA would be interesting. Fourth, the use of different measurement devices, such as OCT, OCTA, and mfERG, may have resulted in errors in the correspondence of the measurement area. However, we believe that this is a realistic and clinically relevant study to analyze the microstructure, microcirculation, and function of the local retina in a layer-by-layer manner.

This study demonstrated the relationship between macular blood supply and macular function in glaucomatous eyes. In glaucomatous eyes, a decrease in N1–P1 amplitude was observed in relation to a reduction in DRL-mVD, indicating that ischemia-induced bipolar cell dysfunction may be involved in intermediate retinal dysfunction associated with glaucoma.

Acknowledgments

The authors thank Editage (https://www.editage.jp) for their English language review.

Supported in part by a grant from the Japan Society for the Promotion of Science (21K16904).

Disclosure: **Y. Yoshikawa**, None; **T. Shoji**, None; **J. Kanno**, None; **H. Ishii**, None; **M. Chino**, None; **Y. Igawa**, None; **K. Shinoda**, None; **Y. Miyake**, None

References

1. Racette L, Wilson MR, Zangwill LM, Weinreb RN, Sample PA. Primary open-angle glaucoma in blacks: a review. *Surv Ophthalmol.* 2003;48(3):295–313.
2. Quigley HA, Broman AT. The number of people with glaucoma worldwide in 2010 and 2020. *Br J Ophthalmol.* 2006;90:262–267.
3. Weinreb RN, Khaw PT. Primary open-angle glaucoma. *Lancet.* 2004;363(9422):1711–1720.
4. Flammer J. The vascular concept of glaucoma. *Surv Ophthalmol* 1994;38(suppl):S3–S6.
5. Flammer J, Orgül S, Costa VP, et al. The impact of ocular blood flow in glaucoma. *Prog Retin Eye Res.* 2002;21(4):359–393.
6. Yanagi M, Kawasaki R, Wang JJ, Wong TY, Crowston J, Kiuchi Y. Vascular risk factors in glaucoma: a review. *Clin Exp Ophthalmol.* 2011;39(3):252–258.
7. Yoshikawa Y, Shoji T, Kanno J, Kimura I, Hangai M, Shinoda K. Optic disc vessel density in nonglaucomatous and glaucomatous eyes: an enhanced-depth imaging optical coherence tomography angiography study. *Clin Ophthalmol.* 2018;12:1113–1119.
8. Numa S, Akagi T, Uji A, et al. Visualization of the lamina cribrosa microvasculature in normal and glaucomatous eyes: a swept-source optical coherence tomography angiography study. *J Glaucoma.* 2018;27(11):1032–1035.
9. Akagi T, Iida Y, Nakanishi H, et al. Microvascular density in glaucomatous eyes with hemifield visual field defects: an optical coherence tomography angiography study. *Am J Ophthalmol.* 2016;168:237–249.
10. Yarmohammadi A, Zangwill LM, Diniz-Filho A, et al. Optical coherence tomography angiography vessel density in healthy, glaucoma suspect, and glaucoma eyes. *Invest Ophthalmol Vis Sci.* 2016;57(9):451–459.
11. Akagi T, Zangwill LM, Shoji T, et al. Optic disc microvasculature dropout in primary open-angle glaucoma measured with optical coherence tomography angiography. *PLoS One.* 2018;13(8):e0201729.
12. Shoji T, Zangwill LM, Akagi T, et al. Progressive macula vessel density loss in primary open angle glaucoma: a longitudinal study. *Am J Ophthalmol.* 2017;182:107–117.
13. Manalastas PIC, Zangwill LM, Daga FB, et al. The association between macula and ONH optical coherence tomography angiography (OCT-A) vessel densities in glaucoma, glaucoma suspect, and healthy eyes. *J Glaucoma.* 2018;27(3):227–232.
14. Yoshikawa Y, Shoji T, Kanno J, et al. Glaucomatous vertical vessel density asymmetry of the temporal raphe detected with optical coherence tomography angiography. *Sci Rep.* 2020;10:6845.
15. Lin F, Li F, Gao K, et al. Longitudinal changes in macular optical coherence tomography angiography metrics in primary open-angle glaucoma with high myopia: a prospective study. *Invest Ophthalmol Vis Sci.* 2021;62(1):30.
16. Ha A, Kim YK, Jeoung JW, Park KH. Ellipsoid zone change according to glaucoma stage advancement. *Am J Ophthalmol.* 2018;192:1–9.
17. Asaoka R, Murata H, Yanagisawa M, et al. The association between photoreceptor layer thickness measured by optical coherence tomography and visual sensitivity in glaucomatous eyes. *PLoS One.* 2017;12(10):e0184064.
18. Choi SS, Zawadzki RJ, Lim MC, et al. Evidence of outer retinal changes in glaucoma patients as revealed by ultrahigh-resolution in vivo retinal imaging. *Br J Ophthalmol.* 2011;95:131–41.
19. Werner JS, Keltner JL, Zawadzki RJ, Choi SS. Outer retinal abnormalities associated with inner retinal pathology in nonglaucomatous and glaucomatous optic neuropathies. *Eye (Lond).* 2011;25(3):279–289.
20. Velten IM, Horn FK, Korth M, Velten K. The b-wave of the dark adapted flash electroretinogram in patients with advanced asymmetrical glaucoma and normal subjects. *Br J Ophthalmol.* 2001;85(4):403–409.
21. Parisi V, Ziccardi L, Centofanti M, et al. Macular function in eyes with open-angle glaucoma evaluated by multifocal electroretinogram. *Invest Ophthalmol Vis Sci.* 2012;53(11):6973–6980.
22. Vincent A, Shetty R, Devi SA, Kurian MK, Balu R, Shetty B. Functional involvement of cone photoreceptors in advanced glaucoma: a multifocal electroretinogram study. *Doc Ophthalmol.* 2010;121(1):21–27.
23. Velten IM, Korth M, Horn FK. The a-wave of the dark adapted electroretinogram in glaucomas: are photoreceptors affected? *Br J Ophthalmol.* 2001;85(4):397–402.
24. Zhang Q, Chen CL, Chu Z, et al. Automated quantitation of choroidal neovascularization: a comparison study between spectral-domain and swept-source OCT angiograms. *Invest Ophthalmol Vis Sci.* 2017;58(3):1506–1513.
25. Otsu N. A threshold selection method from gray-level histograms. *IEEE Trans Syst Man Cybern.* 1979;9(1):62–66.

26. Shoji T, Yoshikawa Y, Kanno J, et al. Reproducibility of macular vessel density calculations *via* imaging with two different swept-source optical coherence tomography angiography systems. *Transl Vis Sci Technol.* 2018;7(6):31.
27. Kato F, Miura G, Shirato S, Sato E, Yamamoto S. Correlation between N2 amplitude of multifocal ERGs and retinal sensitivity and retinal nerve fiber layer thickness in glaucomatous eyes. *Doc Ophthalmol.* 2015;131(3):197–206.
28. Horiguchi M, Suzuki S, Kondo M, Tanikawa A., Miyake Y. Effect of glutamate analogues and inhibitory neurotransmitters on the electroretinograms elicited by random sequence stimuli in rabbits. *Invest Ophthalmol Vis Sci.* 1998;39(11):2171–2176.
29. Hood DC, Frishman LJ, Saszik S, Viswanathan S. Retinal origins of the primate multifocal ERG: implications for the human response. *Invest Ophthalmol Vis Sci.* 2002;43(5):1673–1685.
30. Machida S, Kaneko M, Kurosaka D. Regional variations in correlation between photopic negative response of focal electroretinograms and ganglion cell complex in glaucoma. *Curr Eye Res.* 2015;40(4):439–449.
31. Viswanathan S, Frishman LJ, Robson JG, Walters JW. The photopic negative response of the flash electroretinogram in primary open angle glaucoma. *Invest Ophthalmol Vis Sci.* 2001;42(2):514–522.
32. Viswanathan S, Frishman LJ, Robson JG, Harwerth RS, Smith EL, 3rd. The photopic negative response of the macaque electroretinogram: reduction by experimental glaucoma. *Invest Ophthalmol Vis Sci.* 1999;40(6):1124–1136.
33. Campbell JP, Zhang M, Hwang TS, et al. Detailed vascular anatomy of the human retina by projection-resolved optical coherence tomography angiography. *Sci Rep.* 2017;7:42201.
34. Rao HL, Qasim M, Hussain RS, et al. Structure-function relationship in glaucoma using ganglion cell-inner plexiform layer thickness measurements. *Invest Ophthalmol Vis Sci.* 2015;56(6):3883–3888.
35. Matsushima T, Yoshikawa Y, Shimura A, Yajima A, Ojima Y, Shinoda K. Electrophysiological monitoring of focal and entire retinal function during treatment with intravitreal methotrexate for intraocular lymphoma. *Case Rep Ophthalmol.* 2021;12(1):277–282.
36. Kim EK, Park HL, Park CK. Relationship between retinal inner nuclear layer thickness and severity of visual field loss in glaucoma. *Sci Rep.* 2017;7:5543.
37. Hasegawa T, Akagi T, Yoshikawa M, et al. Microcystic inner nuclear layer changes and retinal nerve fiber layer defects in eyes with glaucoma. *PLoS One.* 2015;10(6):e0130175.
38. Hare WA, Ton H. Effects of APB, PDA, and TTX on ERG responses recorded using both multifocal and conventional methods in monkey. Effects of APB, PDA, and TTX on monkey ERG responses. *Doc Ophthalmol.* 2002;105(2):189–222.
39. Hood DC. The multifocal electroretinographic and visual evoked potential technique. In: Heckenlively JR, Arden GB, eds. *Principles and Practice of Ophthalmology of Vision*. Cambridge, MA: MIT Press, 2006:197–205.